Jour. of the KGS, Vol. 23, No. 3. March 2007, pp. 41~50

Characteristics of Shear Behavior of Remolded Nak-dong River Sandy Silt

재성형된 낙동강 모래질 실트의 전단거동 특성

Kim, Young-Su[1] 김 영 수
Tint, Khin Swe[2] 틴킨스웨
Kim, Dae-Man[3] 김 대 만

요 지

본 논문에서는 실트 함유율이 높은 모래에 대한 정규압밀 등방배수 및 비배수 삼축압축시험(NCIU 및 NCID) 결과를 나타내었다. 유효구속응력 100~400kpa하에서 실트 함유율이 63%인 낙동강 모래 시료를 사용하여 실험을 실시하였다. 실험결과, 모래질 실트는 초기에는 압축이 되지만 전체적인 응력-변형률 곡선에서 최종적으로 체적팽창반응을 보였다. 모래질 실트의 거동은 낮은 소성 특성으로 인하여 점토와 모래보다 비하여 그 특성을 묘사하기가 어려웠다. 특히, 시료는 파괴 후 전단과정에서 팽창현상을 보였다. 모래질 실트의 전단거동과 전단강도정수는 응력-변형률 거동과 Mohr-Coulomb 파괴규준에 의하여 결정되는데, 전단거동은 파괴 후 변형률 연화 경향과 같이 체적변화가 증가하는 것으로 관찰되었다. 본 논문에서 모래질 실트의 전단과정 동안에 발생되는 팽창거동은 모래 함유율 뿐만 아니라 저점착력을 가진 세립자의 함유율에 의해서도 달라졌다.

Abstract

The results from normally consolidated isotropic drained and undrained triaxial compression tests (NCIU and NCID) on sand with high silt content were presented in this paper. The experiments were performed on specimens of Nak-dong River sand with 63% silt content under effective confined pressures, 100 kPa to 400 kPa. From test results, Sandy silt became initially compressive but eventually appeared to provide dilatancy response throughout the entire stress-strain curve. The behavior of sandy silt was more difficult to characterize than that of clay and sand due to lower plastic characteristic. Especially, the samples exhibited dilatancy development during shear after failure. The shear behavior and shear strength parameters of sandy silt can be determined as stress-strain behaviors are described by the Mohr-Coulomb failure criterion. The shear behaviors were observed increasing dilatancy volume change tendency with strain-softening tendency after failure. In this paper, the behavior of dilatancy depends on not only sand content but also fine content with low-cohesion during shear in the samples of sandy silt.

Keywords : Critical state line, Sandy silt, Shear strength, Stress-strain response, Triaxial tests

1 Member, Ph.D., Prof., Dept. of Civil Engrg., Kyungpook National Univ., Korea
2 Doctor Course, Dept. of Civil Engrg., Kyungpook National Univ., Korea, khinswetint@yahoo.com, Corresponding Author
3 Member, Ph.D., Lecturer, Dept. of Civil Engrg., Jinju National Univ., Korea

1. Introduction

The sandy silt is more difficult to characterize than the behavior of clay or sand because of its tendency to dilate during shear and establish a consistent and practically useful failure criterion (Yamamuro 2001). When granular soils contain a certain amount of fines, the characteristics of shear strength vary with fines content. The shear strength parameters of soil for foundation designs essentially require the shear strength of the soil to check the stability and settlements of soil. From the experiment results, the appropriate shear strength parameters that can be used to foundation design are important. The stress-strain curve is significant for safety structure limitation and the development of soil failure depends on the range of stress-strain response obtained from triaxial compression tests. Preparing sandy silt samples for triaxial and consolidation testing without sampling disturbance is very difficult. Disturbance influences the measured shear strength in triaxial tests and obscures the past consolidation pressure in consolidation tests. Sandy silts tend to dilate during shear, and changes in pore water pressure decrease due to strains increase. In this paper, to study the normally consolidated isotropic drained and undrained shear strength behaviors of Nak-dong River sandy silt, series of standard triaxial tests were performed on the soil specimens which isotropically consolidated in the remolded conditions. From the test results, the stress-strain relationship is nonlinear and peak shear strength develops at intermediated axial strain and critical-state shear strength (corresponding to no volume change during shearing) develops with large axial strains after failure. If the pore pressures decrease to values below the vapor pressure of water, cavitations occur and bubbles of air are liberated from the pore water (Brandon 2006). When this happens, shear does not occur at constant volume but the specimens were exhibited with no volume change at critical state in shearing under loading. Normally consolidated tests were carried out for various confining pressures. The soil specimens used in this paper consisted of silt-sand mixtures that include fine-grained surface soils which is defined as ML (sandy silts) according to Unified Classification System (Yilmaz 2004). The samples were sheared to failure under static loading to investigate the strength and deformation response in triaxial compression test. Remolded soils had a significant effect on the stress-strain and pore water pressure behavior under undrained condition. The increment of undrained strength was a result of the reduction in water content that occurred when the remolded sample was consolidated. The strength values in laboratory are higher than the field strength (Fleming 1990). An increase of dilatancy with fines content is related to the greater fines content (Salgado 2000). When granular soils contain a certain amount of fines, the characteristics of shear strength vary with fines content. The focus of the laboratory testing program was to develop shear strength parameters and shear behaviors of drained and undrained consolidated (CD and CU triaxial tests) on Nak-dong River sandy silt. Shear strength parameters and shear behaviors can be determined as the Mohr-Coulomb failure criterion is commonly used to describe shear failure in soils and stress-strain responses. Moreover, the laboratory tests included soil classification, primary consolidation, unit weight, Atterberg limit, saturation and consolidation in triaxial tests.

2. Experimental Methods

2.1 Physical Properties

Atterberg limits tests were performed on the sandy silt to classify the soils and to establish their geotechnical engineering properties after remolding. Laboratory tests in this paper included physical properties and two types of triaxial tests (Consolidated drained and undrained tests). The soil materials were obtained from Nak-dong River in Gumi. The soil was prepared with sieve No.40 and remolded before preconsolidation test. The physical properties of Nak-dong River sandy silt and loose sand are presented in Tables 1 and 2. The soil classifications based on grain-size distribution curve of Nak-dong River sandy silt and loose sand are shown in Figs. 1 (a) and (b). The soil was graded between No.10 and 200 sieve sizes.

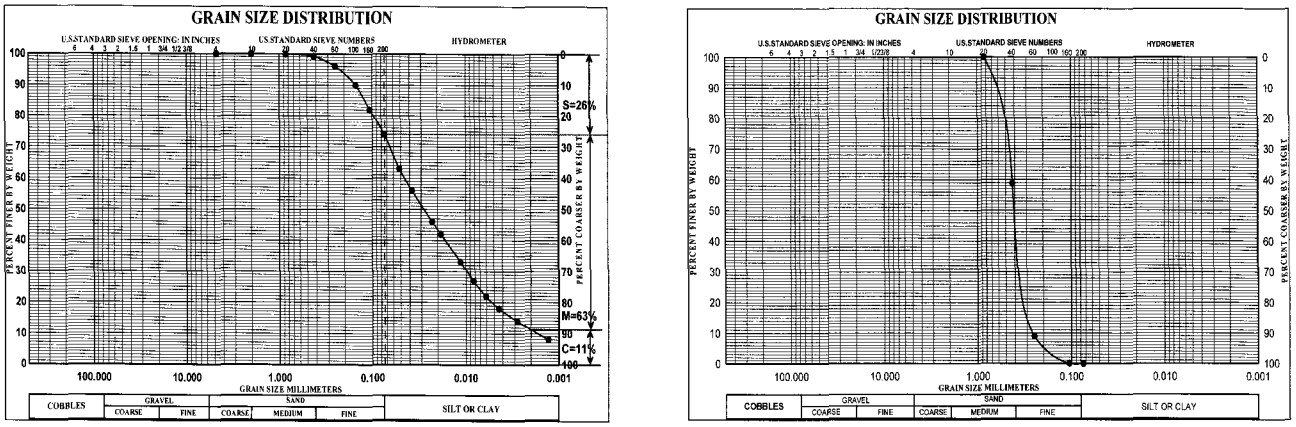

(a) (b)

Fig. 1. Grain size distribution of (a) Nak-dong River sandy silt and (b) loose sand

Table 1. Physical properties of Nak-dong River sandy silt

G_s	D_{60} (mm)	D_{30} (mm)	D_{10} (mm)	C_u	C_z	e_{max}	e_{min}	LL (%)	PI (%)	Sand (%)	Silt (%)	Clay (%)	USCS
2.64	0.045	0.01	0.0018	25	1.235	0.713	0.631	25	6	26	63	11	ML

Table 2. Physical properties and grain sizes of Nak-dong River loose sand

G_s	D_{60} (mm)	D_{30} (mm)	D_{10} (mm)	C_u	C_z	e_{max}	e_{min}	Sand (%)	Silt (%)	Clay (%)	USCS
2.676	0.43	0.37	0.27	1.593	1.179	1.137	0.765	100	0	0	SP

2.2 Primary Consolidation Test

The cylindrical preconsolidation apparatus in diameter 28 cm and height 50 cm is shown in Fig. 2. The sandy silt was provided as a bulk sample which is mixed with water and remolded before testing. The soil slurry was applied to by preconsolidated pressures, 7.5, 15, 30 and 60 kPa respectively during one month. The settlements of preconsolidation test results by using primary pressures step by step are shown in Fig. 3. The primary consolidation test is conducted on a remolded sample of sandy silt. After the sample of sandy silt is set up and an initial small load 7.5 kPa is applied to it, the amount of compression that the soil undergoes is measured over time. Firstly the samples will be compressed rapidly under initial preconsolidation pressure 7.5 kPa as the water flows out of the sample and grains shift position to decrease the size of the voids. Therefore the settlements of samples are very large in the beginning of pressure. Eventually the rate of consolidation will slow and the settlements are not as large as initial stage because the samples start to consolidate under increasing preconsolidation pressure. The height of sample decreased and the settlement happened continuously until constant value of settlement due to consolidation under preconsolidation pressures as shown in Fig. 3. If the settlement is constant under each of preconsolidation pressures, the current consolidation step is ended and the preconsolidation pressure is increased to next step. The total settlements of samples are 14 cm in about one month. The water content is calculated after maximum load was exposed to the soil.

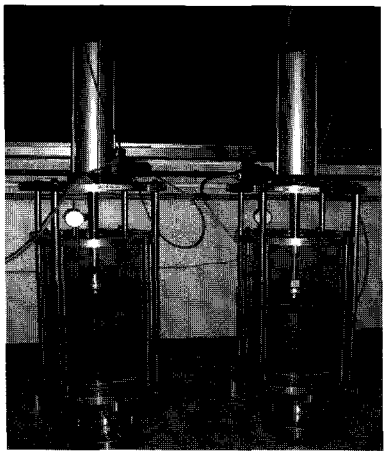

Fig. 2. Preconsolidation test

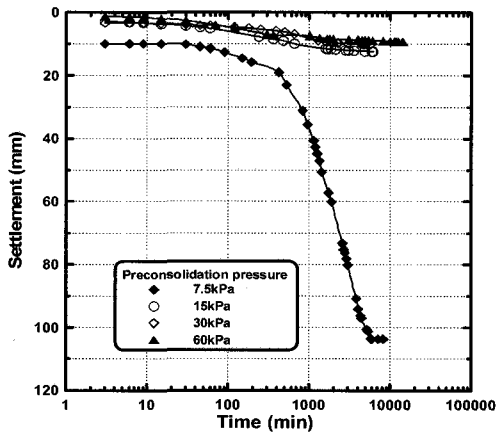

Fig. 3. Settlement and time (log t)

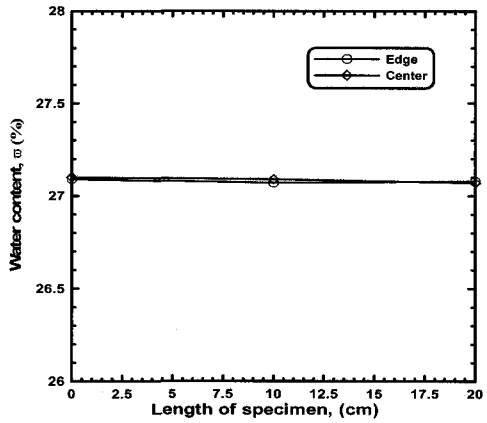

Fig. 4. Water content and length of specimen

Thus some of the soils have been taken from top, middle and bottom layers of center and edge of the preconsolidation sample for checking of water content after preconsolidation test. The values of water content for samples are approximately the same and the soil is approximately homogenous as shown in Fig. 4. The water content was 27.1% and the unit weight of dry density, γ_d is 15.11 kN/m^3 after preconsolidation test. The water content, ω was 74% before preconsolidation test. The sample were extruded and coated with wax prior to triaxial testing.

2.3 Preparation for Specimen and Shear Test

Normally consolidated isotropic drained and undrained triaxial compression tests were performed on cylindrical specimens measuring 50 mm in diameter by 100 mm in height as shown in Fig. 5. The specimens were trimmed as a necessary cylindrical shape before triaxial testing. The void ratio of the test specimens ranged from 0.713 (initial stage) to 0.631 (before shear). The undrained shear strength significantly depends on the initial void ratio and water content of the each sample due to the changing of excess pore water pressure. Water content is little different from among the specimens after preconsolidation test because of taking the setting time for the triaxial test. The saturation of sample was performed by cell pressure, 50 kPa and back pressure, 45 kPa at the beginning and gradually increased during saturation stage until B-value is at least 0.95. A back pressure was used to prevent cavitations of the pore water and to ensure full saturation in all tests (Yamamuro 2004). The effects of membrane penetration and filter paper were not considered significant during shear test because for soft and very soft soil the membrane effect can form an appreciable proportion of the measured strength and for soils of high strength, the effect of the membrane restraint is insignificant and is usually neglected. After saturation stage, the specimens were consolidated under isotropic effective confining pressures, 100, 200, 300 and 400 kPa respectively.

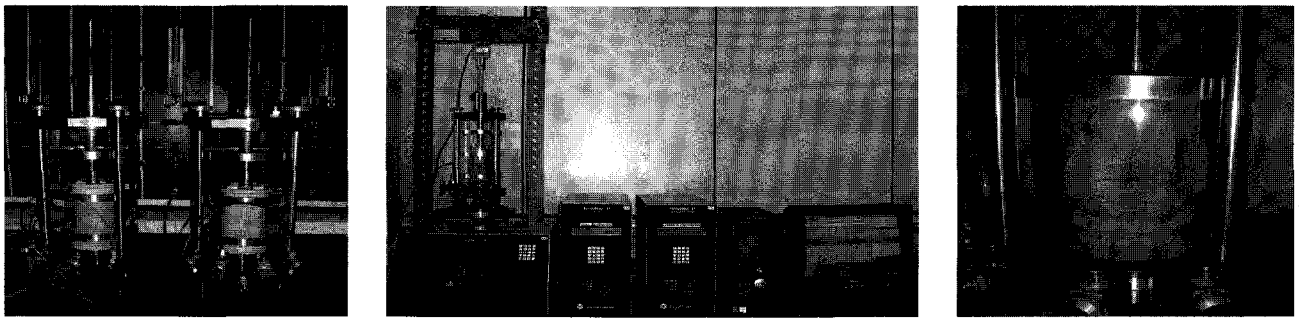

(a) Saturation and consolidation (b) Triaxial shear test (c) shear condition

Fig. 5. Normally consolidated isotropic drained and undrained triaxial test of Nak-dong River sandy silt

Table 3. Normally consolidated isotropic triaxial test

Sample	Conditons	Final effective consolidated stress (kPa)
Sandy silt	NCIU NCID	100 200 300 400

Significant volume changes of specimen may occur particularly during the consolidation. The following Table 3 is presented for normally consolidated isotropic condition of triaxial compression test. Shear strength tests were conducted on the remolded samples of sandy silt after consolidation phase. Normally consolidated undrained and drained tests were performed in strain rate 0.1% per minute and 0.05% per minute under shear condition because the maximum rate of strain to be applied is equal to ε_f/t_f% per minute. The value of t_f which is the time from the start of compression to failure is obtained from $1.8t_{100}$ minutes for CU test and $14t_{100}$ for CD test with side drains (the use of filter paper).

3. Test Results

3.1 Normally Consolidated Isotropic Undrained Tests (NCIU)

In a series of undrained triaxial compression tests, the strength didn't increase with further straining and dilatency because deviator stresses exhibited softening tendency after the specimen statically collapsed. The typical behavior of normally consolidated isotropic undrained triaxial test for Nak-dong river sandy silt is shown in Fig. 6. The deviator stress and axial strain responses are presented in Fig. 6 (a). A stress-strain curve can be delineated into three regions: initial elastic region, hardening region and softening region. The peak of deviator stress is smooth in higher confining pressure and is not presented in lower confining pressure due to the dilatency during undrained shearing. The following distinguishing features are: (1) the peak and the ultimate points of the deviator stresses are one and the same; (2) pore- water pressure buildup is positive; (3) the effective stress path from mean effective

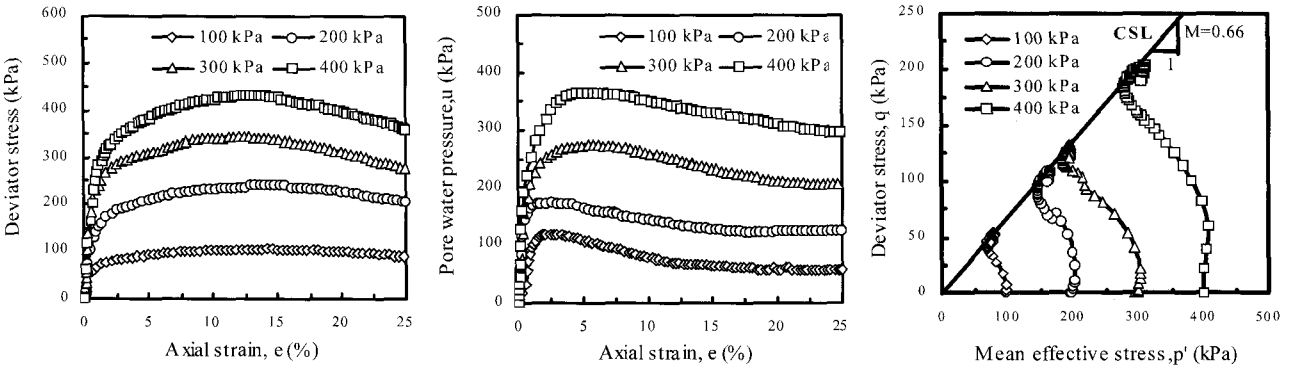

(a) Deviator stress-strain responses (b) Pore water pressure versus axial strain (c) p' versus q

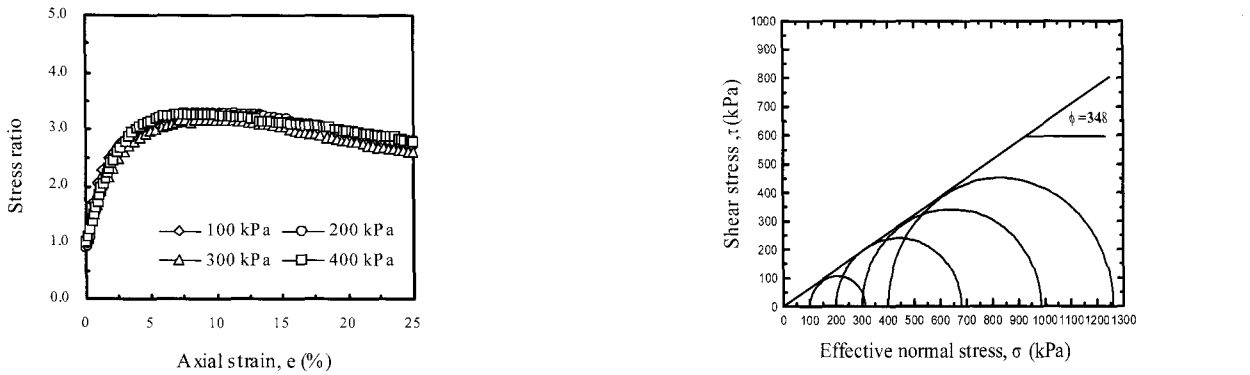

(d) Stress ratio versus axial strain (e) Mohr's circles for shear stress versus effective normal stress

Fig. 6. Results of normally consolidated isotropic undrained triaxial tests for Nak-dong River sandy silt

stress, p'=100, 200, 300 and 400 kPa are approximately geometrically similar; and (4) the failure points lie on a line (the critical state line, CSL) that passes through the origin of the p'-q space (Anandarajah 2000) as shown in Fig. 6 (c). The maximum deviator stresses between σ'_3=100 and 400 kPa are 81.65 kPa (14.56% failure strain), 330.31 kPa (13.01% failure strain) as shown in Fig. 6 (a). Moreover, the plots of deviator stresses are constant under effective confining pressure, σ'_3=100 kPa and showed the softening tendency under σ'_3=200, 300 and 400 kPa after peak deviator stress.

When the deviator stresses increase, the effective vertical stress, σ'_1 decreases and total vertical stress, σ'_1, effective confining pressure, σ'_3 and pore water pressure, u increase and total confining stresses are constant before failure. The pore water pressures decrease and then the void ratio of the samples increase due to dilatant behavior beyond failure during shearing as shown in Fig. 6 (b). All of peak pore water pressures exist between 120 kPa (σ'_3=100 kPa) and 360 kPa (σ'_3=400 kPa) in 2 to 5% failure strain. The maximum pore water pressure is exhibited in small strain and decreased as axial strain increase after critical state. Due to the dilatancy, the bonding tendency among the soil particles is destroyed and happened with no interlocking at failure state. The peak strength of sandy silts is insignificantly influenced by interlocking because the undrained stress paths are different from the drained stress paths that converged toward the right side of each mean effective stress, p' to the critical state line since the excess pore water pressure development is positive (Horpibulsuk 2004). The effective confining stress has major influence in changing the behavior of sandy silt from contractive to dilative. M is a critical state frictional constant, (the slope of the critical state line on a q-p' plot at failure condition) which is a function of ϕ'_{cs} (from M= 6sinϕ/(3-sinϕ)) and essential for critical state model in Fig. 6 (c). The parameter, M(q_f/p'_f) is 0.66. The sample is sheared with constant pore water pressure at the steady or critical state. The effective stress ratios and axial strain are shown in Fig. 6 (d). All of stress ratios declined slightly that the sample exhibited dilatancy after the peak values of stress ratio.

The limiting stress ratio suggests that the true frictional angle should not be changed throughout the stress-strain history. Peak undrained strength followed a lower stress ratio for the critical state condition (Been 2004). According to the normally consolidated undrained triaxial tests, the shear strength increases with the amount of greater silt content owing to higher dilatancy by Salgado (2004). The angle of internal friction, ϕ is 34° and the failure deviator stresses in Mohr's circle are shown in Fig. 6 (e). The shear strength increases due to increasing shear stress with higher effective normal stress in Fig. 6 (e).

3.2 Normally Consolidated Isotropic Drained Tests (NCID)

In four drained triaxial compression tests, there are no distinct peak deviator stress and smooth curve under effective confining pressure, 300 and 400 kPa and then the peak deviator stresses do not appear under effective pressure, 100 and 200 kPa as shown in Fig. 7 (a). The deviator stresses at σ'_3 kPa decreased slightly but these at σ'_3 = 100 to 300 kPa decreased smoothly and showed softening tendency after the peak value of deviator stress in Fig. 7 (a). The peak deviator stresses are between 200 kPa (15% axial strain) at σ'_3 = 100 kPa and 750 kPa (16.25% axial strain) at σ'_3 = 400 kPa. The volumetric strain at σ'_3 = 100 kPa decreased to negative value (i.e. swelling) after failure. The behavior of specimens showed the first strain hardening character at σ'_3 = 200 to 400 kPa because of the (positive) compressive volumetric strains, (i.e. contraction of volume) before failure and the second strain showed a strain-softening tendency due to the expansive volumetric strains (i.e. dilation of volume) after failure in Fig. 7 (b). Based on the test results, the specimens exhibited the decrement of volume under higher confining pressure before failure. The minimum and maximum values of volumetric strains at σ'_3 = 100 kPa and 400 kPa are between 0.05% (4% failure strain) and 0.12% (7.6% failure strain) as shown in Fig. 7 (b).

The results indicated that the failure stress levels, overall trends of the stress-strain behavior and the volume change behavior are significantly influenced by the presence

of silt (Shapiro and Yamamuro 2003). For tests conducted with kPa, the samples at the end of testing were distinctly dilatant and hence critical state had not been approached in volumetric strains. For σ'_3 = 400 kPa, the samples at failure (or the end of test) were closed to constant volume.

Failure deviator stresses exist on a unique line which is a critical state line (CSL) as shown in Fig. 7 (c). The stress paths are similar and converged to the right side of the each mean effective stress towards a critical state line and then all of the failure points terminated at the critical state line in the stress paths diagram. Furthermore, the mean effective stresses and deviator stresses were increased to CSL. The slope of critical state line in the stress paths is denoted by *M*, a material parameter which is 0.49. When the specimen of soil reaches a critical state, the sample is sheared continuously and causes failure as constant shear stress and no volume change tendency with increasing shear strain (Boukpeti 2000). The frictional angle ϕ is 29° as shown in Fig. 7 (d).

It is possible to trace the stress paths of the specimens during shearing in the tests to determine if the stress paths would eventually reach the extended Mohr-Coulomb failure envelope which is significant for the shear strength of specimens (Rahardjo 2004). According to the analysis of test results, the volume of sample tends to decrease because the void ratio is smaller with higher confining pressures and the strength increases as the effective normal stress increases before critical state. When the deviator stresses hardened, the effective vertical stress, σ'_1 and total vertical stress, σ'_1, also increased and then the effective confining pressure, σ'_3, total confining stress, σ'_3 are constant with increasing axial strain before failure. When the deviator stresses softened, the effective vertical stress, σ'_1 and the total vertical stress, σ'_1, decrease after

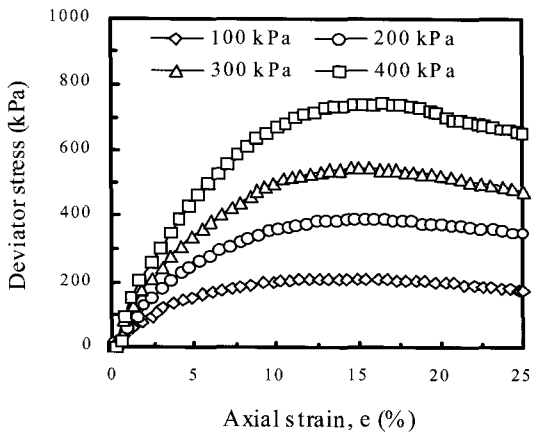

(a) Deviator stress-strain response

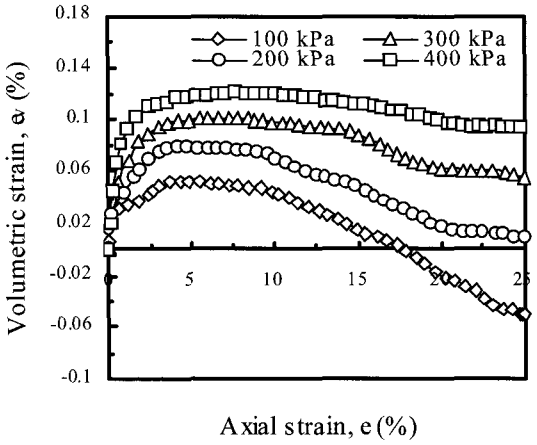

(b) Volumetric strain versus axial strain

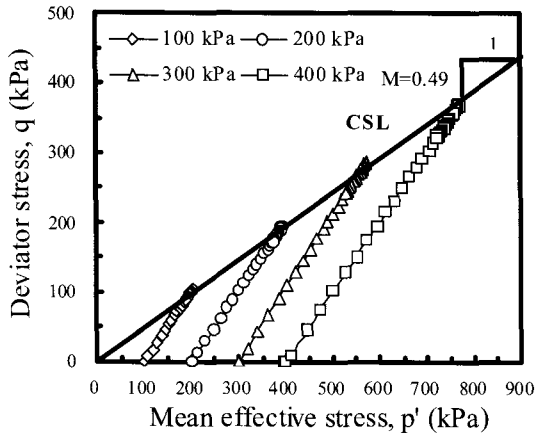

(c) p' versus q

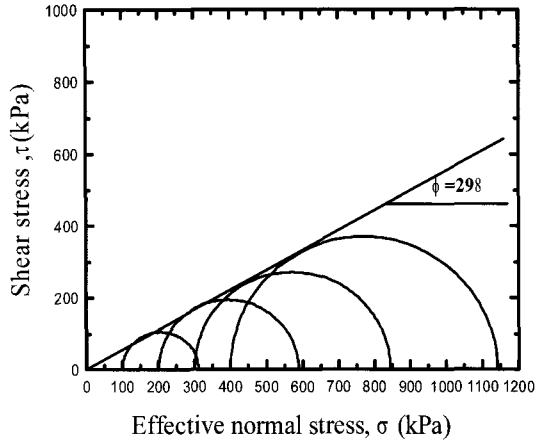

(d) Mohr's circles

Fig. 7. Normally consolidated isotropic drained triaxial tests results of Nak-dong River sandy silt

failure condition during shearing. From these results, tests were conducted for compression at lower confining stress during the initial stage of shearing before failure.

4. Comparison of Undrained Nak-Dong River Sandy Silt with Loose Sand

According to the undrained test results of shear strength of loose sand as shown in Fig. 8, the framework of understanding is stress-dilatancy theory because the pore water pressure showed negative value after maximum pore water pressure. The samples of saturated loose sand were sheared to failure and showed only a hardening tendency and a significant decrease in pore water pressure due to the increment of effective stress and strength and then deviator stresses of sandy silt showed softening tendency after failure in stress-strain response. The loose sands do not increase in volume to failure (Been 2004) and tend to dilate due to development of the negative pore water pressure (i.e. swelling of volume) after critical state (Pestana 2002). The sandy silts exhibited only positive value of pore water pressure which decreased slowly after failure and showed a little dilation behavior. In stress-strain behavior of sand and sandy silt, the critical state is the same as the failure state in sand because there is no peak deviator stress. However, the peak deviator stress of sandy silt appears under higher confining pressure and then the critical state is the same as the failure state at lower confining pressure similar to loose sand behavior. In sand, critical state typically occurs after effective stress failure at large strains. At the critical state, all samples remain constant values of pore water pressure and effective stresses at large strains (Yamamuro 1998). Deviator stresses of sand are more than those of sandy silt at σ'_3 = 100 to 300 kPa except 400 kPa. Moreover, the deviator stress of sand hardened at small strain within 0.5% and that of sandy silt increased stiffly at large strain within 2.5% at the beginning condition. The maximum failure strain of pore water pressures of sandy silt is 5% and 2% in loose sand. The pore water pressure of sand has more softening tendency than that of sandy silt which showed only positive value but pore pressure of sand happened to be negative values after failure. The failure deviator stresses, q of sandy silt are shorter length than these of sand on the critical state line. The peak values of q with maximum

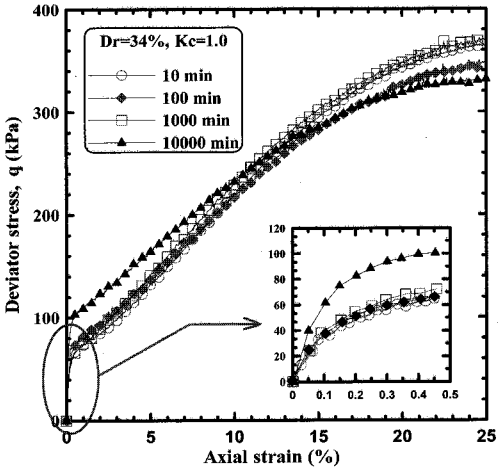

(a) Deviator stress versus axial strain

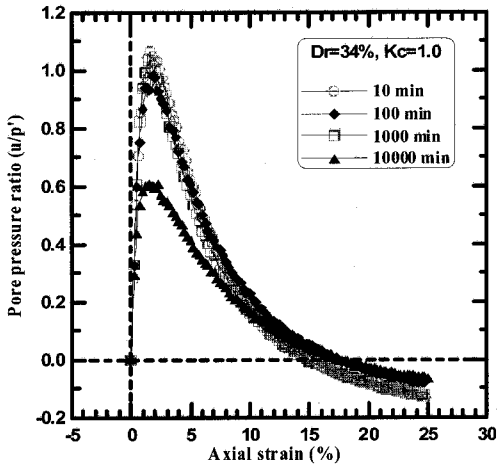

(b) Pore water pressure versus axial strain

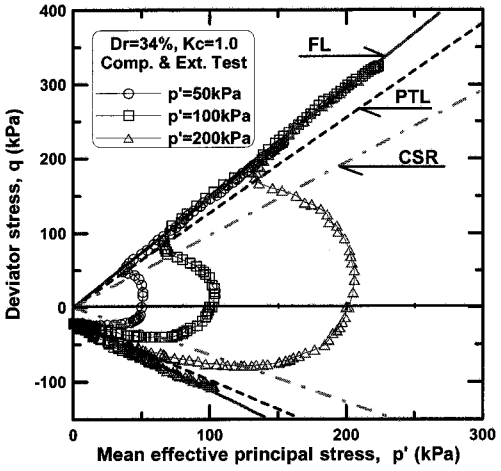

(c) Stress paths

Fig. 8. Results of laboratory tests using Nak-dong River loose sand (Kim Young-Su, 2004)

effective confining pressures are 200 kPa of sandy silt and 400 kPa of sand on the failure line in stress paths. All of failure deviator stresses followed to a critical state line (CSL) when specimens of sandy silt and loose sand are sheared. From analysis of results, deviator stress of normally consolidated sandy silt is failure at 12.5% strain but loose sands didn't exhibit the failure exactly.

5. Conclusions

Analysis of the experimental study on Nak-dong River sand with high silt content was conducted. From the laboratory test results of normally consolidated isotropic undrained of sandy silt, the deviator stress increased to peak value as a strain-hardening tendency until failure and showed strain-softening tendency after failure. Peak deviator stresses are not distinct and smooth under increasing effective confining pressure and not appeared under lower effective confining pressure. Pore water pressure decreased and exhibited as the dilative behavior of the samples after failure during shearing. Stress paths converged to the left side of the each mean effective stress towards the critical state line. Stress ratios decreased and presented a unique line and dilatancy of sample with increasing axial strain after failure. Shear stresses increase under higher effective confining pressure. Undrained shear behavior of sandy silt showed dilatancy and the shear strength increased with higher effective normal stress.

Normally consolidated drained triaxial compression tests of Nak-dong River sandy silt also indicated that deviator stresses at failure were constant for σ'_3 = 100 kPa hence the sample approached to the critical state. However, for tests conducted with σ'_3 = 100, 200 and 300 kPa, the deviator stresses were softened at the end of testing so that the critical state had not been approached after failure. The initial strain before failure hardened up to peak value and exhibited compression volumetric strains and then the final strain after failure softened and presented expansive volumetric strains under various effective confining pressures after failure condition. Stress paths converged to the right side of the each mean effective stress towards the critical state line. Drained shear behavior of sandy silt exhibited more dilatancy with lower effective confining pressure and the shear strength increased with shear stress and the effective normal stress.

Nak-dong River sandy silt and sand have different behaviors in normally consolidated isotropic undrained tests. The deviator stress of sand with small strain and sandy silt with large strain increased stiffly at the initial condition during shear.

From analysis of these results, the deviator stress of sandy silt showed strain-softening tendency after failure but loose sand exhibited a strain-hardening tendency until the end of test. There are no peak deviator stresses in sand but the peak deviator stresses of sandy silt appeared smoothly under high confining pressure until failure. The pore water pressure of sandy silt showed only positive value but pore pressure of sand was exhibited by decreasing to negative after failure. The failure deviator stresses of sandy silt are shorter than that of sand along the critical state line. All of the stress paths are similar in each test and all failure deviator stresses followed to a unique line which is a critical state line (CSL) or steady state line in stress path diagram.

The axial strain for peak strength of the interlocked structure of soil specimens increases with confining pressure. The strength derived from the interlocking increases with increasing confining pressure. If we consider soil properties in terms of effective stress, the most marked feature of which the failure criterion must take account is the increment of strength as the effective stress increases. The pore water pressure build-up is reduced under undrained loading and undrained strength increase in stress paths diagram. The dilation component contributes to a portion of total strength whereas for the higher effective confining stress, the strength after the peak is dominated by dilation with lower plasticity.

References

1. Anandarajah, A. (2000), "Triaxial behavior of kaolinite in different pore fluids", *J. Geotech. Eng.*, ASCE, Vol.126, No.2, pp.148-156.
2. Been Ken and Jefferies Michael (2004), "Stress-dilatancy in very loose sand", *Can. Geotech. J.*, Vol.41, pp.972-989.
3. Boukpeti, N. (2000), "Triaxial behavior of refined Superior sand

model", *Computer and Geotechnics. J.*, Vol.26, pp.65-81.
4. Brandon Thomas L., Rose Andrew T. (2006), "Drained and undrained strength interpretation for low-Plasticity silts", *J. Geotech. Engrg*, ASCE, Vol.132, No.2, pp.250-257.
5. Fleming Lorraine N. (1990), "Stress-deformation characteristics of Alaskan silt", *J. Geotech. Eng.*, ASCE, Vol.116, No.3, pp.377-393.
6. Horpibulsuk Suksun (2004), "Undrained shear behavior of cement admixed clay at high water content", Vol.130, No.10, pp.1096-1105.
7. Lee Junhwan, Salgado Rodrigo (2004) "Stiffness degradation and shear strength of silty sands", *Can. Geotech. J.*, Vol.4, pp.831-843.
8. Lo S.R. and Wardani S.P.R. (2002) "Strength and dilatancy of a silt stabilization by a cement and fly ash mixture", *Can. Geotech. J.*, Vol.39, pp.77-89.
9. Pestana Juan M. (2002), "Evaluation of a constitutive model for clays and sands : Part I-sand behavior", *Int. J. Numer. Anal. Meth. Geomech.*, Vol.26, pp.1097-1121.
10. Rahardjo, H. (2004), "Shear strength of a compacted residual soil from consolidated drained and constant water content triaxial tests", *Can. Geotech. J.*, Vol.41, pp.421-435.
11. Salgado, R. (2000), "Shear strength and stiffness of silty sand", *J. Geotech. Eng.*, ASCE, Vol.126, No.5, pp.451-462.
12. Shapiro Saul (2003) "Effect of silt on three-dimensional stress-strain behavior of loose sand", *J.Geotech. Engrg.*, ASCE, Vol.129, No.1, pp.1-11.
13. Yamamuro Jerry A., Kelly M. Covert (2001), "Monotonic and cyclic liquefaction of very loose sands with high silt content", *J. Geotech. Eng.*, ASCE, Vol.127, No.4, pp.314-324.
14. Yamamuro Jerry A. and Lade Poul V. (1998), "Steady-state concepts and static liquefaction of silty sands", *J.Geotech. Engrg.*, ASCE, Vol.124, No.9, pp.868-877.
15. Yamamuro Jerry A., Wood Fletcher M. (2004), "Effect of depositional method on the undrained behavior and microstructure of sand with silt", *Soil dynamics and Earthquake Eng.*, Vol.24. pp.751-760.
16. Yilmaz, M.T. (2004), "Undrained cyclic shear and deformation behavior of silt-clay mixtures of Adapazari, Turkey", *Soil dynamics and Earthquake Eng.*, Vol.24, pp.497-507.
17. Young-Su Kim, Dae-Man Kim (2004), "Characteristics of Undrained static Shear Behavior for Sand Due to againg effect", *J. Geotech. Eng.*, KGS, Vol.20, No.6, pp.137-150.

(received on Sep. 28, 2006, accepted on Jan. 31, 2007)